

RESEARCH

Open Access



Astrocytes carrying LRRK2 G2019S exhibit increased levels of clusterin chaperone *via* miR-22-5p and reduced ability to take up α -synuclein fibrils

Alice Filippini^{1†}, Giulia Carini^{1,2†}, Alessandro Barbon², Massimo Gennarelli^{1,2} and Isabella Russo^{1,2*} 

Abstract

Accumulating evidence highlights that dysfunction of astrocyte biology might contribute to Parkinson's disease (PD) onset and progression. Leucine-rich repeat kinase 2 (*LRRK2*), a gene linked to genetic and familial PD, has been reported to affect astrocytic-related functions, including the ingestion of alpha-synuclein (α -syn) aggregates. In this context, we recently showed that the extracellular chaperone clusterin (Clu) binds to and limits the uptake of alpha-syn fibrils by astrocytes. Thus, starting from these premises, we explored whether LRRK2 G2019S affects aggregated α -syn ingestion through the Clu-related pathway and the underlying molecular mechanisms. We first validated in our LRRK2 G2019S knock-in (KI) mouse strain that primary astrocytes exhibited an impaired ability to ingest fibrillary α -syn. Then, we investigated whether LRRK2 G2019S affects this pathway through the modulation of Clu. In this regard, we collected several results showing that LRRK2 regulates Clu levels in astrocytes. Specifically, brain slices and primary astrocytes from KI mice with the LRRK2 G2019S pathological mutation exhibit increased levels of Clu protein compared to their respective wild-type (WT). Accordingly, we observed an opposite effect in brain slices and primary astrocytes from LRRK2 knock-out (KO) mice in comparison to their respective WT. To gain insights into the molecular mechanism underlying LRRK2-dependent Clu modulation, we found that LRRK2 controls Clu expression at the translation level through the action of miR-22-5p. In addition, we demonstrated that treatment with miR-22-5p mimic improves the ability of LRRK2 G2019S-KI astrocytes to take up α -syn pffs. Taken together, our findings indicate that the LRRK2-Clu pathway is involved in the ingestion of α -syn fibrils and that the impairment of α -syn uptake in LRRK2 G2019S-KI astrocytes is associated to Clu levels. Future studies will allow us to understand whether the modulation of astrocytic LRRK2 G2019S-Clu pathway might attenuate the neuronal spreading of α -syn pathology in PD.

Keywords LRRK2, Clusterin, Parkinson's disease, Astrocytes, miRNA

[†]Alice Filippini and Giulia Carini contributed equally to this work.

[†]Alice Filippini and Giulia Carini contributed equally to this work.

*Correspondence:

Isabella Russo
isabella.russo@unibs.it

¹IRCCS Istituto Centro San Giovanni di Dio Fatebenefratelli, Brescia, Italy

²Unit of Biology and Genetics, Department of Molecular and Translational Medicine, University of Brescia, Brescia, Italy



© The Author(s) 2025. **Open Access** This article is licensed under a Creative Commons Attribution-NonCommercial-NoDerivatives 4.0 International License, which permits any non-commercial use, sharing, distribution and reproduction in any medium or format, as long as you give appropriate credit to the original author(s) and the source, provide a link to the Creative Commons licence, and indicate if you modified the licensed material. You do not have permission under this licence to share adapted material derived from this article or parts of it. The images or other third party material in this article are included in the article's Creative Commons licence, unless indicated otherwise in a credit line to the material. If material is not included in the article's Creative Commons licence and your intended use is not permitted by statutory regulation or exceeds the permitted use, you will need to obtain permission directly from the copyright holder. To view a copy of this licence, visit <http://creativecommons.org/licenses/by-nc-nd/4.0/>.

Introduction

Parkinson's Disease (PD) is one of the most common neurodegenerative diseases worldwide, characterized by progressive neuronal death occurring in several brain regions, including the *substantia nigra pars compacta* [10, 11]. The main hallmarks of PD are the Lewy bodies and Lewy neurites, typical neuronal protein inclusions mainly composed of aggregated and insoluble α -syn [11, 52]. Emerging evidence reported that aggregated α -syn can be released by stressed and degenerated neurons, leading to the neuron-to-neuron spreading of toxic aggregates through the brain [3, 9, 32]. Thus, the uptake/clearance of extracellular α -syn aggregates might be beneficial to prevent α -syn propagation and the progression of the pathology. Recent literature highlights that astrocytic dysfunctions might play an important role in the development and progression of α -syn pathology. In this regard, it has been reported that astrocytes are able to ingest extracellular aggregated α -syn [15, 31, 54, 57], and, interestingly, we specifically showed that the chaperone clusterin (Clu) interferes with α -syn fibrils uptake [15], making the modulation of this pathway interesting to be further explored. In addition to Clu, a number of PD-related genes, such as *Leucine-rich repeat kinase 2* (*LRRK2*), have been shown to alter the endo-lysosomal pathway and affect the clearance of α -syn species [14]. Thus, based on these observations, in this study, we investigated whether *LRRK2* G2019S affects α -syn uptake through the Clu-related pathway, and we shed light on the underlying molecular mechanisms.

LRRK2 is a large multimeric kinase protein associated with familial PD and sporadic cases as a risk factor [44, 50, 62]. Among *LRRK2* pathological mutations, the G2019S is the most frequent and accounts for about 40% of familial cases in certain populations and 1–2% of idiopathic PD cases [4, 22, 36]. *LRRK2* has been linked to multiple cellular pathways, including cytoskeletal dynamics, translation, inflammation, and vesicle trafficking [5, 37, 49]. From the expression standpoint, *LRRK2* is expressed in different tissues and organs, with high expression in the brain and particularly in astrocytes [25, 49]. As reported above, accumulating evidence associates *LRRK2* with the clearance of α -syn in both brain phagocytic cells, microglia, and astrocytes. Specifically, microglia with *LRRK2* deficiency exhibited an enhanced clearance of α -syn [34]. Accordingly, astrocytes carrying *LRRK2* G2019S reported reduced capacity to take up and degrade α -syn aggregates [12, 54]. Taken together, these results indicate that *LRRK2* controls the ingestion/clearance of α -syn in glial cells; however, the intracellular signaling(s) orchestrated by *LRRK2* remain largely unknown.

In this study, we first validated in our transgenic mouse strain that primary astrocytes carrying the

LRRK2 G2019S mutation exhibited an impaired ability to ingest extracellular α -syn fibrils, and then we investigated whether *LRRK2* G2019S could affect this pathway through the chaperone Clu. Intriguingly, we found that brain slices and primary astrocytes from *LRRK2* G2019S knock-in (KI) mice displayed increased levels of Clu protein compared to their respective wild-type (WT). Accordingly, we showed an opposite effect in the brain slices and primary astrocytes from *LRRK2* knock-out (KO) mice. At the molecular level, we observed that *LRRK2* regulates Clu at the translational step *via* miR-22-5p. In addition, we demonstrated that treatment of *LRRK2* G2019S-KI astrocytes with miR-22-5p mimic can improve the ability of astrocytes to take up α -syn aggregates. Overall, our results indicate that *LRRK2* G2019S impacts the uptake of α -syn aggregates by astrocytes through Clu and suggest that *LRRK2* G2019S-Clu pathway might be targetable to promote astrocytic α -syn clearance and consequently attenuate the neuronal spreading of α -syn pathology in PD.

Materials and methods

Animals and primary astrocytes

Animals were maintained under a 12-hour light-dark cycle at room temperature (RT, 22 °C) and had *ad libitum* food and water. Constitutive C57BL/6 N *LRRK2* KO and their respective WT mice were obtained from Dr. Claudia Lodovichi (C57BL/6-*Lrrk2*^{tm1.1Mjff}/J; strain #016121). While constitutive C57BL/6J *LRRK2* G2019S-KI mice with their respective WT were acquired from Jackson Laboratory (B6.Cg-*Lrrk2*^{tm1.1Hlme}/j; strain #030961). In this study we used homozygous for both genotypes (homozygous KO/KO and homozygous KI/KI). All procedures were performed in accordance with European Community Directive 2010/63/UE and approved by the Ministry of Health (Project ID: 800-2017-PR; and 211B5.N.TMW).

Primary astrocytes were derived from postnatal days 1–4 (P1–P4) and generated as recently reported [15]. Briefly, cerebral cortices were dissociated in cold PBS, the cell suspension was then allowed to settle for 5 min at RT, and the top fraction was collected and centrifuged for 5 min at 190 RCF. Subsequently, the cells were resuspended in complete astrocyte medium containing DMEM high glucose (ThermoFisher Scientific), 10% fetal bovine serum (FBS, ThermoFisher Scientific), 2 mM L-glutamine (ThermoFisher Scientific), and Penicillin/Streptomycin (ThermoFisher Scientific). Cell suspension obtained from five brains was plated on T175 flasks and maintained in culture until confluence (DIV7–9), when the cells were processed for experimental applications. The purity grade of primary astrocytic culture was verified by immunostaining with CD11b and GFAP antibodies, microglial and astrocytic markers, respectively.

Generation of α -syn pre-formed fibrils (pffs) and cell treatment

Human monomeric α -syn protein (kindly provided by Prof. L. Bubacco, University of Padova, Italy) was incubated for 14 days at 37 °C under constant shaking to induce aggregation. Pre-formed fibrils (pffs), isolated by the soluble part of the preparation by centrifugation at 15,340 RCF for 15 min at RT, were then quantified relative to the initial concentration of monomer before fibrillation, as previously described [15, 46, 48], and resuspended in PBS. While mouse α -syn pffs were acquired by StressMarq (SPR-324). pHrodo-labeled α -syn pffs were generated by using the pHrodo™ iFL Green Microscale Protein Labeling kit (ThermoFisher Scientific), as recently reported [15].

Primary astrocytes were treated with pHrodo-labeled α -syn pffs at 2 μ M for 16 h, as previously published [15]. Quantification of intracellular α -syn pffs was performed using ImageJ software. Specifically, after removal of the background intensity, the intracellular α -syn pffs was calculated as the fluorescence intensity of all the cell divided by cellular area and expressed as fluorescence intensity/ μ m². At least fifty cells were randomly chosen in a minimum of three independent experiments. Results are shown as cumulative frequency distribution (%). Images were acquired with a Zeiss Axioplan2 fluorescence microscope with a 63 \times oil-immersion objective (Carl Zeiss AG).

SUnSET assay

To measure protein synthesis levels in primary astrocytes, we used the SUnSET (SURface SENSing of Translation) assay by using puromycin [20, 51]. Puromycin is a structural analogue of the tyrosyl-transfer RNA that can be incorporated into elongating peptide chains, leading to puromycin-labeled peptides, which reflect the overall rate of protein synthesis [51]. To this aim, we treated astrocytes with 1 μ M puromycin for 30 min, and then we analyzed the amount of labeled-puromycin peptides in the cell lysates through western blotting by using an anti-puromycin antibody.

Cell Lysis and Western blotting

Astrocytes were washed twice with 1X PBS, solubilized with cold lysis buffer (20 mM Tris-HCl pH 7.5, 150 mM NaCl, 1 mM EDTA, 2.5 mM sodium pyrophosphate, 1 mM β -glycerophosphate, 1 mM Na₃VO₄, 1% Triton-X-100, protease inhibitors), incubated on ice for 20 min, and centrifuged at 15,340 RCF at 4 °C. The supernatant was collected for protein electrophoresis. Specifically, total proteins were separated using 7.5% acrylamide Sodium Dodecyl Sulphate (SDS)-PAGE gels. Subsequently, proteins were transferred on a polyvinylidene difluoride (PVDF) membrane (Bio-Rad), saturated

with 5% non-fat dry milk in 1% TBS-Tween (TBST) for 1 h at RT, and incubated with primary antibodies: anti-Clu (R&D System, AF2747, 1:1000), anti-GAPDH (ThermoFisher Scientific MA5-15738, 1:30000), anti-LRRK2 (Abcam, ab133474, MJFF2 1:300), anti-Puromycin (Millipore, MABE343 1:1000), anti-phospho-4E-BP (Thr37/46, Cell Signaling, #9459), and anti-4E-BP (Cell Signaling, #9452). Next, membranes were incubated with Horseradish Peroxidase (HRP)-conjugated secondary antibodies (Merck-Sigma Aldrich) for 1 h at RT and then with ECL substrate of HRP (GE healthcare).

Brain immunostaining

For all the experiments performed *ex vivo* we used 13-month-old mice since it has been shown that animal models with LRRK2 deletion or mutations develop LRRK2-mediated phenotypes with aging [1, 25, 55, 61]. For the immunostaining, after dissection, the brain tissue was washed in cold PBS and then fixed with 4% PFA. After 10 days of post-fixation, brains were transferred to a 30% sucrose solution, and then sectioning was started once the brains had sunk to the bottom. The brains were then cut into 40 μ m thick coronal sections and stored in the antifreeze solution (0.5 M phosphate buffer, 30% glycerol, and 30% ethylene glycol) at -20 °C until used for immunostaining analysis. For immunostaining, sections were washed with PBS and incubated for 1 h in the blocking solution (5% FBS, 0.3% Triton in PBS). Afterwards, primary antibodies anti-Clu (R&D Systems, AF2747, 1:100) and anti-GFAP (Invitrogen, 13-0300, 1:500) were incubated ON at 4 °C in the blocking solution. The next day, sections were washed three times with PBS and incubated with AlexaFluor conjugated secondary antibodies for 1 h at RT. After three washes with PBS, sections were mounted using Prolong Gold Antifade reagent containing DAPI (ThermoFisher Scientific), and images were taken using a Zeiss LSM 510 confocal microscope equipped with a Zeiss 63 \times /1.4 numerical aperture oil-immersion objective (Carl Zeiss AG) at the Imaging Platform of the Department of Translational and Molecular Medicine at the University of Brescia.

RNA extraction, retro-transcription, and real-time PCR

Total RNA from primary astrocytes was extracted using the ZymoResearch™ kit (Irvine, CA, USA), according to the manufacturer's instructions. Then, the retro-transcription reaction was performed using Moloney Murine Leukemia Virus-Reverse Transcriptase (MMLV-RT, ThermoFisher Scientific). Briefly, 500 ng of total RNA were mixed with 2 μ L of 0.3 μ g/ μ L random primers (ThermoFisher), 8 μ L of 5 \times buffer (ThermoFisher Scientific), 2 μ L of 10 mM dNTPs (ThermoFisher Scientific), 4 μ L of 0.1 M DTT (ThermoFisher Scientific), 2 μ L of 40 U/ μ L RNaseOUT (ThermoFisher Scientific), and 2 μ L

MMLV-RT (200 U/ μ L, ThermoFisher Scientific) in a final volume of 40 μ L. The reaction mixture was incubated at 37 °C for 2 h, and then the enzyme was inactivated at 75 °C for 10 min.

To analyze *Clu* expression, we used the ViiA™ 7 Real-time PCR system (ThermoFisher Scientific) with Taqman probes and the universal PCR Master Mix (Life Technologies) following the manufacturer's instructions. We used the following probes: *Clu* (ID: Mm01197002_m1), *GAPDH* (ID: Mm99999915_g1) and *H2AFz* (ID: Mm02018760_g1) as housekeeping (HK) genes. The relative expression of *Clu* was calculated using the comparative Ct ($\Delta\Delta$ Ct) method, normalized on the geometric mean of the two HK genes, and expressed as Fold Change (rq).

miRNAs selection

microRNAs (miRNAs) targeting *Clu* mRNA were predicted according to four online databases, including miRDB (<https://mirdb.org/mirdb/index.html>) [8], TargetScan (https://www.targetscan.org/mmu_80/) [40], miRWalk (<http://mirwalk.umm.uni-heidelberg.de/>) [53], and TarBase v.8 (<https://dianalab.e-ce.uth.gr/html/diana/web/index.php?r=tarbasev8%2Findex>) [27]. By integrating the results, miRNAs that were simultaneously predicted by at least three different databases were selected for further validation (Suppl. Table 1).

RNA extraction, miRNA retro-transcription, and real-time PCR

Total RNA from primary astrocytes and striatum of 13-month-old mice was extracted using the ZymoResearch™ kit (Irvine, CA, USA), according to the manufacturer's instructions. Reverse transcription was carried out using miRCURY® LNA® RT kit (QIAGEN, Milano, Italy). Briefly, 100 ng of total RNA were mixed with 2 μ L of 5x miRCURY RT SYBR® Green Reaction Buffer and 1L of miRCURY RT Enzyme Mix in a final volume of 10 μ L. The reaction mixture was incubated at 42 °C for 1 h, and then the enzyme was inactivated at 95 °C for 5 min. qPCR was performed using the ViiA™ 7 Real-time PCR system (ThermoFisher Scientific) with the miRCURY® LNA® miRNA PCR assay (QIAGEN, Milano, Italy) and the iTaq Universal SYBR Green supermix (Bio-Rad Laboratories, Milano, Italy) following the manufacturer's instructions. We used the following primers for the qPCR: miR-15b-5p (YP00204243), miR-16-5p (YP00205702), miR-22-5p (YP00204255), miR-195-5p (YP00205869), miR-497a-5p (YP00205164), miR-3059-3p (YP02116190), miR-6999-5p (YP02119107), miR-7054-5p (YP02111351), miR-7073-5p (YP02110075) and 5 S rRNA (YP00203906), RNU1A1 (YP00203909), RNU5G (YP00203908), SNORD68 (YP00203911) and U6 snRNA (YP00203907) for reference RNAs. The relative expression of miRNAs

was calculated using the comparative Ct ($\Delta\Delta$ Ct) method, normalized on the geometric mean of three reference RNAs (5 S rRNA, RNU5G, SNORD68) in astrocytes and of five reference RNAs for the brain lysates (5 S rRNA, RNU1A1, RNU5G, SNORD68 and U6 snRNA), and expressed as rq.

Luciferase assay

For miRNA-mRNA interaction validation, sequences spanning 30 bp before and after the miR-22-5p binding site within the 3' untranslated region (3' UTR) of *Clu* were cloned into the pmirGLO Dual-Luciferase expression vector (Promega; [42]) using the following oligonucleotides: top-TCGAGCTAATGCCTGCACTTGCTGCTCTCGGGAAGAAGACTGATTCCCCCACGCAACTAATCCAATT and bottom-CTAGAATTGGATTAGTTGCTGGGGGAATCAGTTCTTCCCGAGAGCAGCAAGTGCAGGCATTAGC and then validated by sequencing. Dual Luciferase® Reporter assay (E1910, Promega) was used according to the manufacturer's protocol. Specifically, the day before transfection, HEK293T cells were plated in antibiotic-free DMEM medium and then co-transfected with pmirGLO construct vector and 20nM miR-22-5p mimic (MSY0004629 - Syn- miR-22-5p, Qiagen) or the negative control (SI03650318|S1 - All-Stars Negative Control siRNA, NC, Qiagen) using Lipofectamine2000 (0.12 μ L/well 96; Life technologies). 24 h post-transfection, Firefly luciferase activity was measured by reading luminescence (0.1s) with an EnSight™ Multi-mode Plate Reader (PerkinElmer). Firefly luciferase signal was normalized on Renilla signal and expressed as relative luciferase activity.

Cell transfection

Primary astrocytes were transfected with the miR-22-5p mimic or the NC using Magnetofection™ Technology (Oz Biosciences), in accordance with the protocol of the manufacturer. Briefly, 50 nM miR-22-5p mimic or NC were incubated with NeuroMag (NM) magnetic beads (Oz Biosciences; ratio 1 μ g miR:3.5 μ L NeuroMag) for 20 min, then added drop-by-drop to the cells and incubated on a magnetic plate for 15 min at 37 °C. After 1 h, a complete change of medium was performed. 24 h post-transfection, astrocytes were processed for RNA extraction, protein lysates or α -syn pffs treatment as reported above.

Statistical analysis

All data were expressed as mean \pm SEM and represent at least three sets of experiments. All data have been tested for the normality test (Shapiro-Wilk test) before to perform parametric or nonparametric tests. The statistical significance of differences between two groups was assessed by unpaired t-test, one-sample t-test or Mann Whitney test, while for multiple comparisons a one-way

ANOVA followed by Tukey's post-hoc test was used. Cumulative frequency distributions were compared with the Kolmogorov-Smirnov test. Data were analyzed using Prism software (GraphPad), and statistical significance was taken at $p < 0.05$.

Results

Primary astrocytes carrying LRRK2 G2019S exhibit an impaired ability to take up α -syn fibrils

Increasing evidence associates LRRK2 with astrocytic functions, even in relation to α -syn clearance and pathology [12, 54]. In this context, we recently showed that Clu chaperone interferes with the uptake of aggregated α -syn by astrocytes [15]. To investigate whether LRRK2 G2019S could impact α -syn uptake even through the Clu-related pathway, we started this study by validating in our mouse strains the ability of LRRK2 G2019S astrocytes to ingest exogenous fibrillary α -syn. To this end, we generated primary astrocytes from LRRK2 WT and G2019S-KI mice, and we examined α -syn uptake by using the pHrodo-labeled α -syn pffs (Fig. 1a). As shown in Fig. 1b, the cumulative frequency distribution analysis reveals that LRRK2 G2019S-KI astrocytes exhibit intracellular α -syn fluorescence that consistently shifted toward lower intensity values with respect to LRRK2 WT cells, indicating a reduced amount of intracellular α -syn in LRRK2 G2019S-KI cells. Our results are in line with previous findings [54] and, importantly, suggest that an impaired α -syn ingestion by LRRK2 G2019S astrocytes might lead to an higher concentration of α -syn in the extracellular space, which could contribute to the spreading of α -syn pathology.

LRRK2 G2019S-KI mouse brains and primary astrocytes displayed increased levels of chaperone Clu

We previously showed that the chaperone Clu binds to and limits the ingestion of extracellular α -syn pffs by astrocytes [15]. Starting from these premises, we asked whether the reduced uptake of α -syn pffs observed in LRRK2 G2019S-KI astrocytes might be related to Clu modulation. To this aim, we first explored Clu expression in LRRK2 WT and G2019S-KI brain slices by immunostaining. Of interest, we observed increased levels of Clu in LRRK2 G2019S-KI mice compared to their respective WT, mainly expressed by astrocytes (Fig. 2a), which represent the main source of the chaperone in the brain [17, 43, 45]. As reported in the literature, we confirmed that Clu is predominantly expressed by astrocytes by performing immunostaining on mouse brain section and primary cultures of the different brain cell-types (neuron, microglia, and astrocytes; Suppl. Figure 1). Based on these observations, we then asked whether Clu was modulated by LRRK2 G2019S specifically in astrocytic cells. Thus, we generated primary astrocytes from

LRRK2 WT and G2019S-KI mice, and we assessed Clu levels. As shown in Fig. 2b-c, we observed an increase of all Clu forms in G2019S-KI astrocytes compared to WT cells, specifically the intracellular precursor (pre-Clu) and cleaved form (Clu; α and β chains) (Fig. 2b), and the extracellular released form in the medium (Fig. 2c). Taken together, these results indicate that LRRK2 might be a regulator of Clu expression and that the G2019S mutation increases the levels of Clu in astrocytes.

LRRK2 KO mouse brains and primary astrocytes displayed reduced levels of Clu

To confirm the impact of LRRK2 G2019S on the regulation of Clu expression, we took advantage of LRRK2 KO models, specifically mouse brain and their derived primary cultures. In details, we evaluated Clu expression in LRRK2 WT and KO brain sections and primary astrocytes as previously evaluated for ex vivo and in vitro systems from LRRK2 G2019S-KI mice. Interestingly, we found a reduction of Clu levels in both LRRK2 KO brains (Fig. 3a), and primary astrocytes (Fig. 3b-c) compared to the respective WT, supporting the notion that LRRK2 is a positive regulator of Clu expression in astrocytes.

LRRK2 does not affect Clu gene expression

In order to understand how LRRK2 G2019S regulates Clu levels, we first investigated whether LRRK2 was able to affect Clu gene expression. To explore this hypothesis, we performed real-time PCR experiments in LRRK2 G2019S-KI and LRRK2 KO primary astrocytes, each genotype compared to its relative WT. Interestingly, we did not observe a significative difference in Clu gene expression in LRRK2 G2019S-KI compared to WT cells (Fig. 4a); instead, we found that LRRK2 KO astrocytes reported a slight increase in Clu expression compared to their respective WT (Fig. 4b), likely due to a compensatory mechanism for the strong reduction of the protein levels. Taken together, these results indicate that LRRK2 G2019S does not impact Clu at the level of gene expression.

LRRK2 modulates protein translation in astrocytes

We next asked whether LRRK2 G2019S could affect Clu levels through regulation of protein translation in astrocytes. In this regard, it has been shown that LRRK2 is implicated in the protein translation process by affecting ribosomal proteins or translation factors in *Drosophila* and in human and murine neurons [26, 29, 38, 39]. Based on these observations, we performed a SUNSET assay on primary astrocytes generated from both genotypes, LRRK2 G2019S-KI and LRRK2 KO mice. Interestingly, the immunoblot for puromycin revealed that LRRK2 KO astrocytes exhibit a reduced amount, while LRRK2 G2019S-KI cells display an increased amount, of global

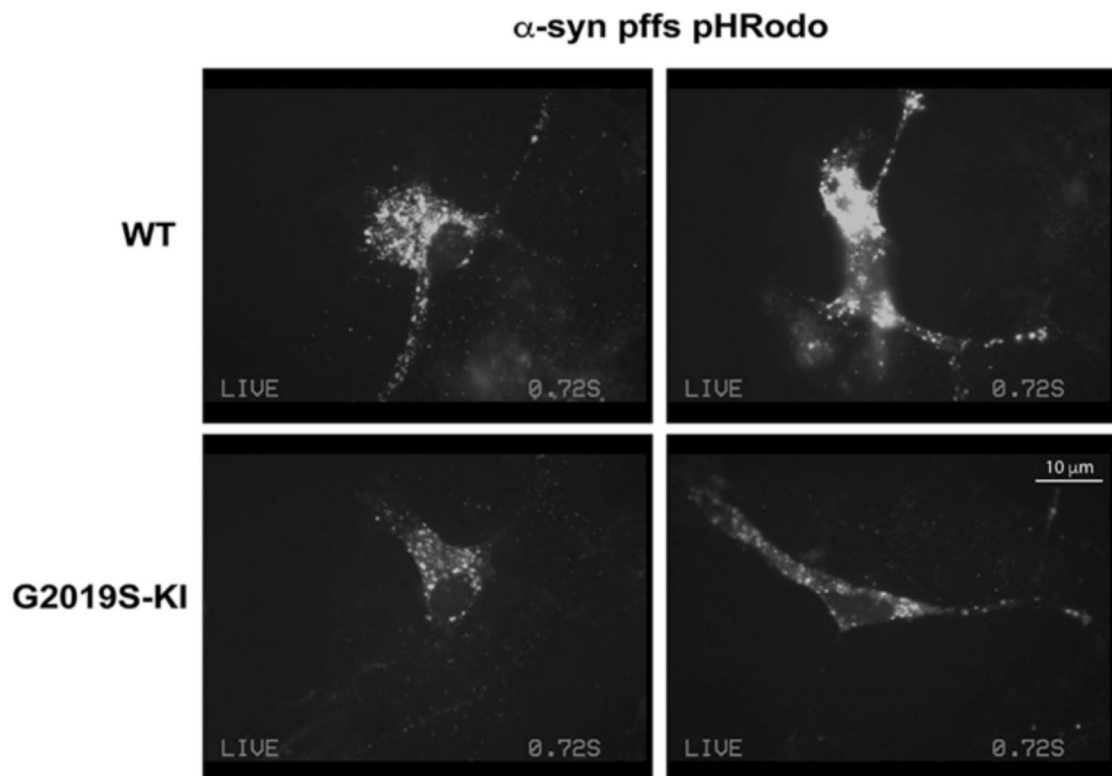
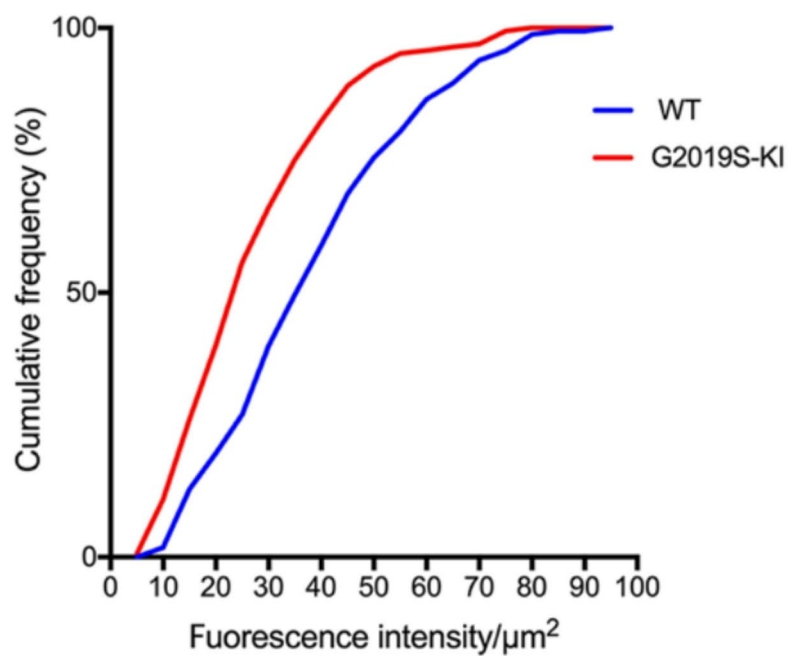
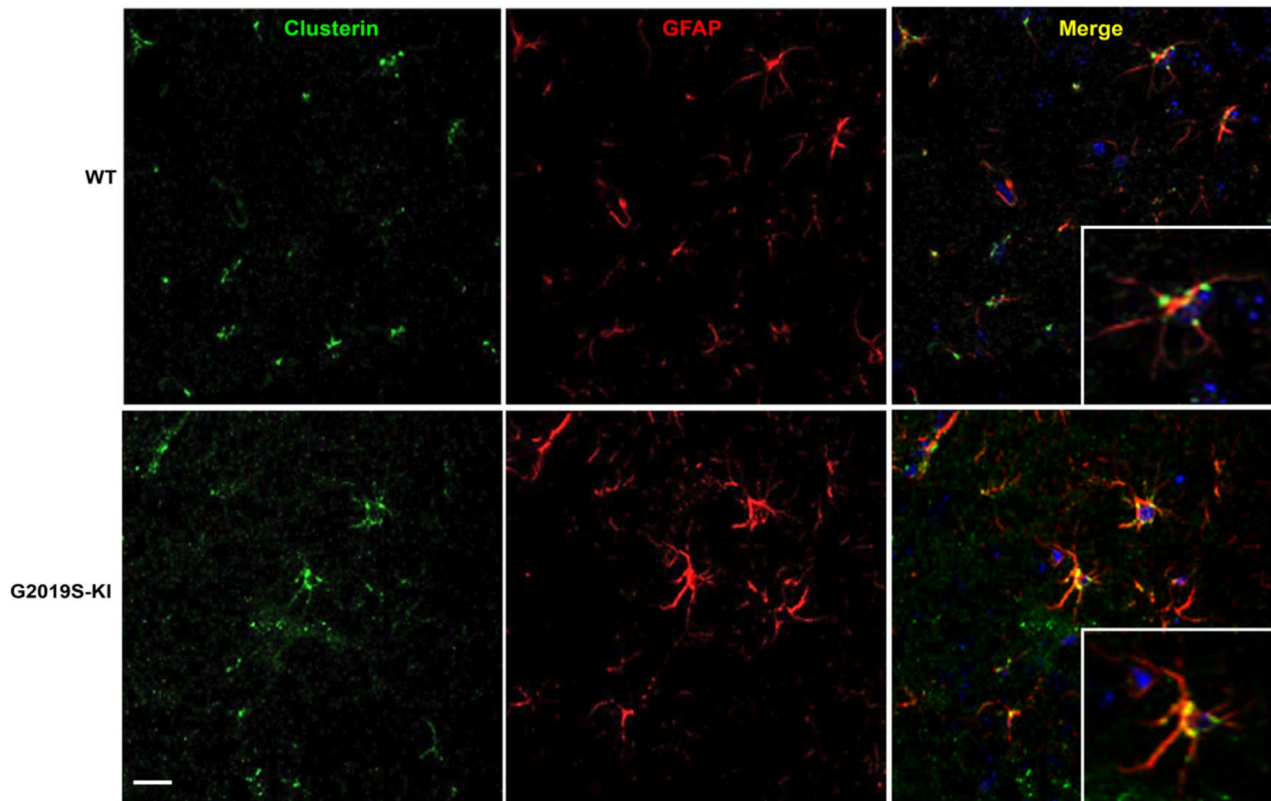
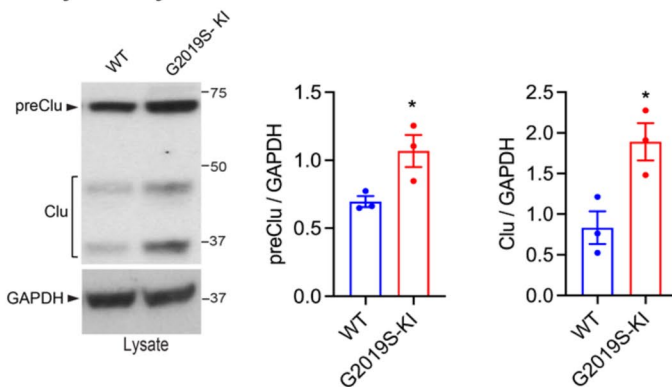
a**b**

Fig. 1 LRRK2 G2019S-KI astrocytes exhibit reduced ability to take up α -syn fibrils. **(a)** Representative fluorescence microscopy images of LRRK2 WT and G2019S-KI astrocytes treated with pHRedo labeled α -syn pffs for 16 h. Scale bar 10 μ m. **(b)** Cumulative frequency distributions of intracellular pHRedo labeled α -syn pffs in LRRK2 WT and G2019S-KI astrocytes (LRRK2 WT = 163 cells and G2019S-KI = 165 cells; Kolmogorov-Smirnov test, $p < 0.0001$). Quantification of intracellular α -syn pffs is calculated as fluorescence intensity/ μ m² from three independent experiments (~50 cells per experiment)

a Mouse brain



b Primary astrocytes



c Primary astrocytes

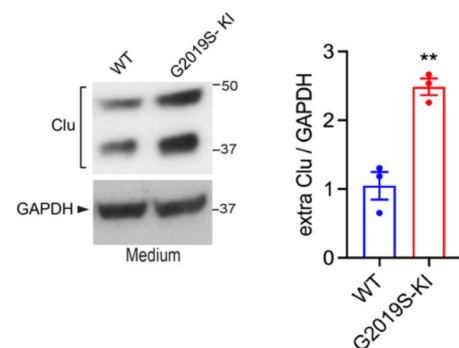


Fig. 2 LRRK2 G2019S-KI brain slices and primary astrocytes exhibited increased levels of Clu protein. **(a)** Maximum Intensity Z-projection confocal images of LRRK2 G2019S-KI and WT brains (13-months old mice) stained for Clu (green), GFAP (red) and nuclei with DAPI (blue). Scale bar 20 μ m. **(b)** Cell lysates of LRRK2 G2019S-KI and WT primary astrocytes were subjected to immunoblotting using Clu and GAPDH antibodies. Data are representative of three independent experiments and are expressed as the mean \pm SEM. Data were analyzed using unpaired t-test; preClu: $p=0.0405$ and Clu: $p=0.0257$. **(c)** Medium from LRRK2 G2019S-KI and WT primary astrocytes were subjected to immunoblotting using Clu antibody. Quantification of extracellular Clu is normalized to GAPDH protein of cell lysates. Data are representative of three independent experiments and are expressed as the mean \pm SEM. Data were analyzed using unpaired t-test; $p=0.0035$

protein synthesis compared to their relative WT cells (Fig. 5a, b), indicating that LRRK2 affects the process of protein translation even in astrocytes. Then, we explored whether LRRK2 G2019S impacts the eukaryotic initiation factor 4E (eIF4E)-binding protein (4E-BP), as recently

shown in *Drosophila* [26]. Thus, we analyzed the levels of LRRK2-mediated phosphorylation 4E-BP in LRRK2 WT and G2019S-KI primary astrocytes; however, we did not find any differences between the two groups analyzed (Fig. 5c). Taken together, our results suggest that LRRK2

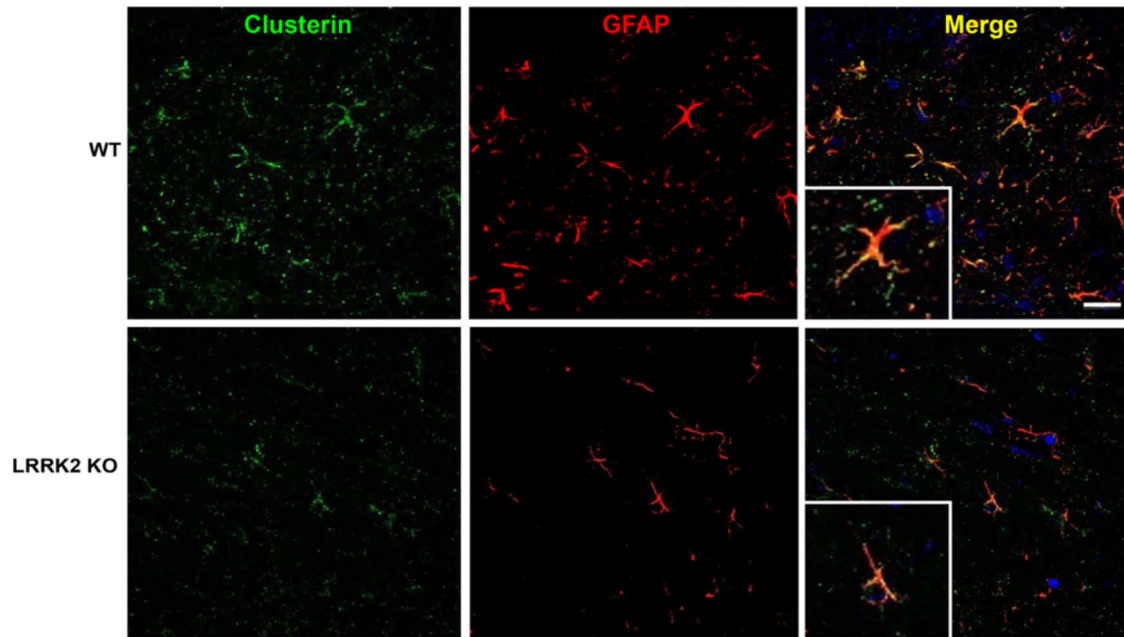
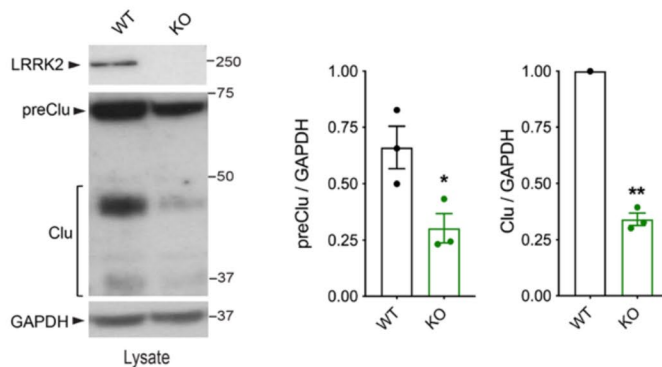
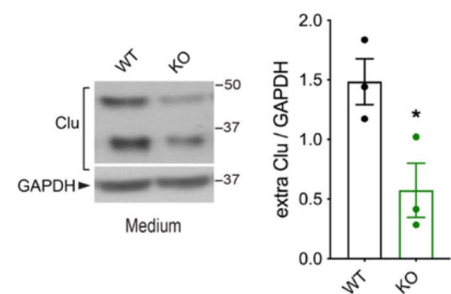
a Mouse brain**b Primary astrocytes****c Primary astrocytes**

Fig. 3 LRRK2 KO mouse brains and primary astrocytes exhibited reduced levels of Clu protein. **(a)** Maximum Intensity Z-projection confocal images of LRRK2 KO and WT brains (13-months old mice) stained for Clu (green), GFAP (red) and nuclei are stained with DAPI (blue). Scale bar 20 μ m. **(b)** Cell lysates of LRRK2 KO and WT primary astrocytes were subjected to immunoblotting using Clu and GAPDH antibodies. Data are representative of three independent experiments and are expressed as the mean \pm SEM. Data were analyzed using unpaired t-test for preClu ($p=0.0353$) and one-sample t-test for intracellular cleaved Clu ($p=0.0017$). **(c)** Medium from LRRK2 KO and WT primary astrocytes were subjected to immunoblotting using Clu antibody. Quantification of extracellular Clu is normalized to GAPDH protein of cell lysates. Data are representative of three independent experiments and are expressed as the mean \pm SEM. Data were analyzed using unpaired t-test; $p=0.0378$

G2019S might modulate Clu levels through regulation of protein translation, but without affecting the translation factor 4E-BP.

LRRK2 modulates Clu protein levels through the action of miR-22-5p

Previous works have shown that LRRK2 is associated with the miRNA pathways to regulate protein translation [18, 19]. Therefore, we explored whether LRRK2 G2019S controls Clu translation in astrocytes through the regulation of specific microRNAs (miRNAs). To this

aim, we queried four online databases, including miRDB, TargetScan, miRWalk, and TarBase, to identify predicted miRNAs that target Clu mRNA. As reported in Fig. 6, the bioinformatics prediction analysis identified 19 miRNAs from miRDB, 74 from TargetScan, 1181 from miRWalk, and 11 from TarBase (Fig. 6a; Suppl. Table 1). Of these, we selected miRNAs that were present in at least three different databases for further investigation (Fig. 6b). Specifically, the following 8 miRNAs were predicted by TargetScan, miRDB, and miRWalk (miR-15b-5p, miR-22-5p, miR-195a-5p, miR-497a-5p, miR-3059-3p,

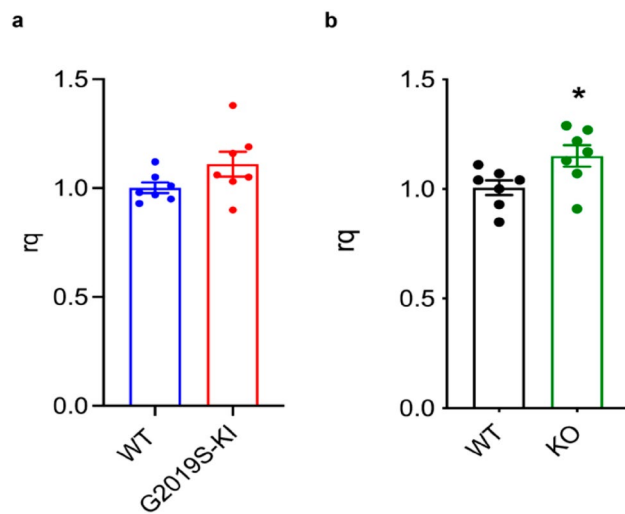


Fig. 4 LRRK2 does not affect Clu gene expression. **(a)** Quantification of Clu gene expression in LRRK2 G2019S-KI and WT primary astrocytes. The relative expression of Clu was calculated using the comparative Ct ($\Delta\Delta C_t$) method, normalized on the geometric mean of the two HK genes, and expressed as fold change (rq). Data are representative of seven independent experiments performed on two different primary cultures and are expressed as the mean \pm SEM. **(b)** Quantification of Clu gene expression in LRRK2 KO and WT primary astrocytes. The relative expression of Clu was calculated using the comparative Ct ($\Delta\Delta C_t$) method, normalized on the geometric mean of the two HK genes, and expressed as rq. Data are representative of seven independent experiments performed on two different primary cultures and are expressed as the mean \pm SEM. Data were analyzed using unpaired t-test, $p=0.0317$

miR-6999-5p, miR-7054-5p, miR-7073-5p), and miR-16-5p was predicted by TarBase, TargetScan, and miRDB (Suppl. Table 1; Fig. 6a, b).

We started analyzing the expression profiles of the 9 selected miRNAs in the primary astrocytes generated from LRRK2 KO and G2019S-KI mice (Fig. 6c, d). Among all, miR-3059-3p, miR-6999-5p, and miR-7073-5p were undetectable in these cells; thus, we continued our investigation with the remaining 6 miRNAs. We found a significant up-regulation of miR-22-5p and miR-497-5p in LRRK2 KO astrocytes compared to their controls (Fig. 6c), while G2019S-KI astrocytes reported a reduction in the expression of miR-15b-5p, miR-16-5p and miR-22-5p when compared with their relative controls (Fig. 6d). Taken together, the miRNAs expression profile proposes miR-22-5p as a putative miRNA for Clu modulation, which is specifically up-regulated in LRRK2 KO astrocytes and down-regulated in LRRK2 G2019S-KI cells. To confirm these results, we analyzed the expression of the 6 selected miRNAs in the striatum of LRRK2 KO mice (one of the regions more affected in PD; Fig. 6e). In detail, LRRK2 KO tissues exhibited a significant increment in the expression of miR-15b-5p and, importantly, of miR-22-5p, further suggesting that miR-22-5p could be the miRNA that controls Clu levels. In order to validate that Clu was targeted by miR-22-5p, we

first implemented the miRNA target binding validation through the luciferase reporter assay. Thus, we cloned the Clu 3'UTRs containing the miR-22-5p binding site into pmirGLO Dual-Luciferase expression vector and we co-transfected it in HEK293 cells with miR-22-5p mimic or with the NC. As shown in Fig. 7b, miR-22-5p mimic treatment significantly decreased firefly luciferase activity compared to NC, thus indicating the direct binding of miRNA-22-5p to Clu mRNA. In addition, we confirm the ability of miR-22-5p mimic to down-modulate the endogenous expression levels of Clu in primary astrocytes. To this aim, we transfected primary astrocytes with miR-22-5p mimic or the NC, and we analyzed Clu at the level of gene expression (Fig. 7d) and protein (Fig. 7e) 24 h post-transfection. Interestingly, we found a strong reduction of preClu and its cleaved form at the protein level, and not at the level of gene expression, in astrocytes transfected with miR-22-5p mimic compared to cells transfected with the NC. Taken together, these results indicate that miR-22-5p controls preClu levels and consequently its cleaved forms.

LRRK2 G2019S-KI astrocytes treated with miR-22-5p mimic exhibited increased ability to take up α -syn pffs

Eventually, we investigated if the treatment with miR-22-5p mimic was able to enhance the ability of LRRK2 G2019S-KI astrocytes to take up α -syn pffs. Thus, we treated primary LRRK2 G2019S-KI astrocytes with the miR-22-5p mimic or the NC for 24 h, then we exposed the cells to pHrodo-labeled α -syn pffs and we examined the amount of intracellular α -syn (Fig. 8a). As shown in Fig. 8b, the cumulative frequency distribution analysis reveals that LRRK2 G2019S-KI astrocytes treated with miR-22-5p exhibit intracellular α -syn fluorescence that consistently shifted toward higher intensity values with respect to cells treated with the NC, indicating an increased amount of intracellular α -syn in LRRK2 G2019S-KI cells treated with miR-22-5p mimic. These results suggest that the impairment of α -syn uptake in LRRK2 G2019S-KI astrocytes is associated to Clu levels.

Discussion

The progressive neuropathological damage seen in PD is thought to be related to the cell-to-cell propagation of aggregated forms of α -syn through the brain. α -Syn aggregates released from stressed/degenerating neurons in the extracellular space represent one of the ways of α -syn spreading between neurons [3, 9, 32]. Interestingly, microglia and recently even astrocytes have been identified as the main scavengers of the Central Nervous System (CNS) [14, 56], able to ingest and clear pathological α -syn species [15, 46–48]. Thus, an interesting point to understand is whether the improvement of glial functions during the disease might represent a beneficial

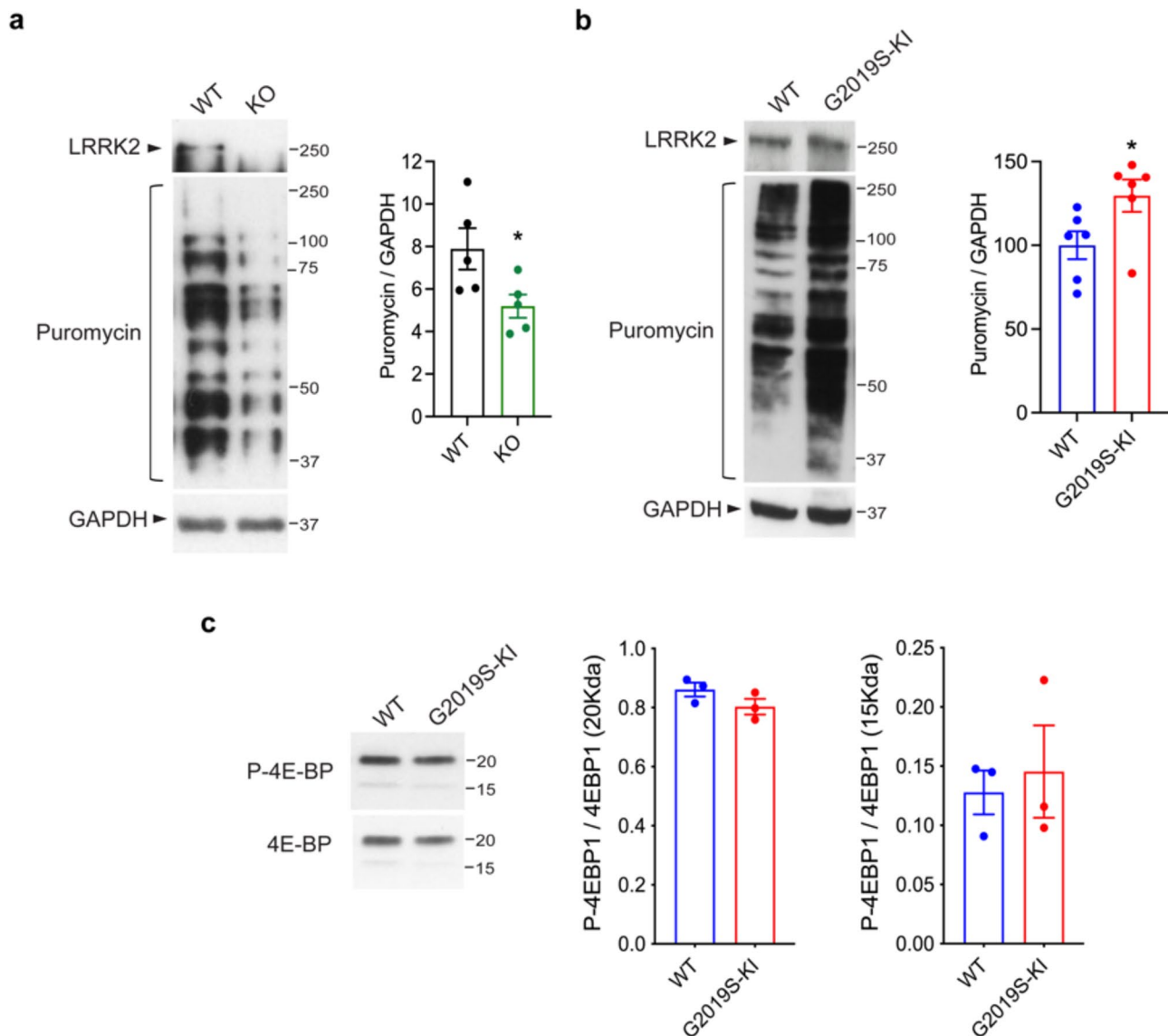


Fig. 5 LRRK2 controls protein translation in astrocytes without affecting the translation factor 4E-BP. **(a)** Cell lysates of LRRK2 KO and WT primary astrocytes previously treated with 1 μ M puromycin for 30 min were subjected to immunoblotting using LRRK2, puromycin and GAPDH antibodies. Data are representative of five independent experiments performed on two different primary cultures and are expressed as the mean \pm SEM. Data were analyzed using unpaired t-test; $p=0.0420$. **(b)** Cell lysates of LRRK2 WT and G2019S-KI primary astrocytes previously treated with 1 μ M puromycin for 30 min were subjected to immunoblotting using puromycin, LRRK2 and GAPDH antibodies. Data are representative of six independent experiments performed on two different primary cultures and are expressed as the mean \pm SEM. Data were analyzed using Mann Whitney test; $p=0.0260$. **(c)** Cell lysates of LRRK2 G2019S KI and WT primary astrocytes were subjected to immunoblotting using P-4E-BP and total 4E-BP antibodies. Data are representative of three independent experiments and are expressed as the mean \pm SEM

strategy to counteract the propagation of α -syn toxic forms between neurons and thus the progression of PD. In this context, our recent study showed that the extracellular Clu chaperone interferes with the uptake of α -syn fibrils by human and murine astrocytes [15]. Moreover, of relevance, we found that the reduction of Clu levels by siRNA technology enhances the ability of astrocytes to ingest α -syn aggregates, revealing that the modulation of this pathway is interesting to be further explored as an

approach to promote α -syn clearance by glial cells and potentially attenuate α -syn spreading and pathology.

Given that LRRK2 takes part in different glia-related cellular pathways, including clearance of misfolded proteins [16, 49], and has been reported to be highly expressed in astrocytes of both mouse and human ex vivo brains [25, 41], in this study we explored whether LRRK2 G2019S might regulate astrocytic ingestion of α -syn *via* Clu. By using murine ex vivo brains and primary cultures, we observed that LRRK2 positively regulates the

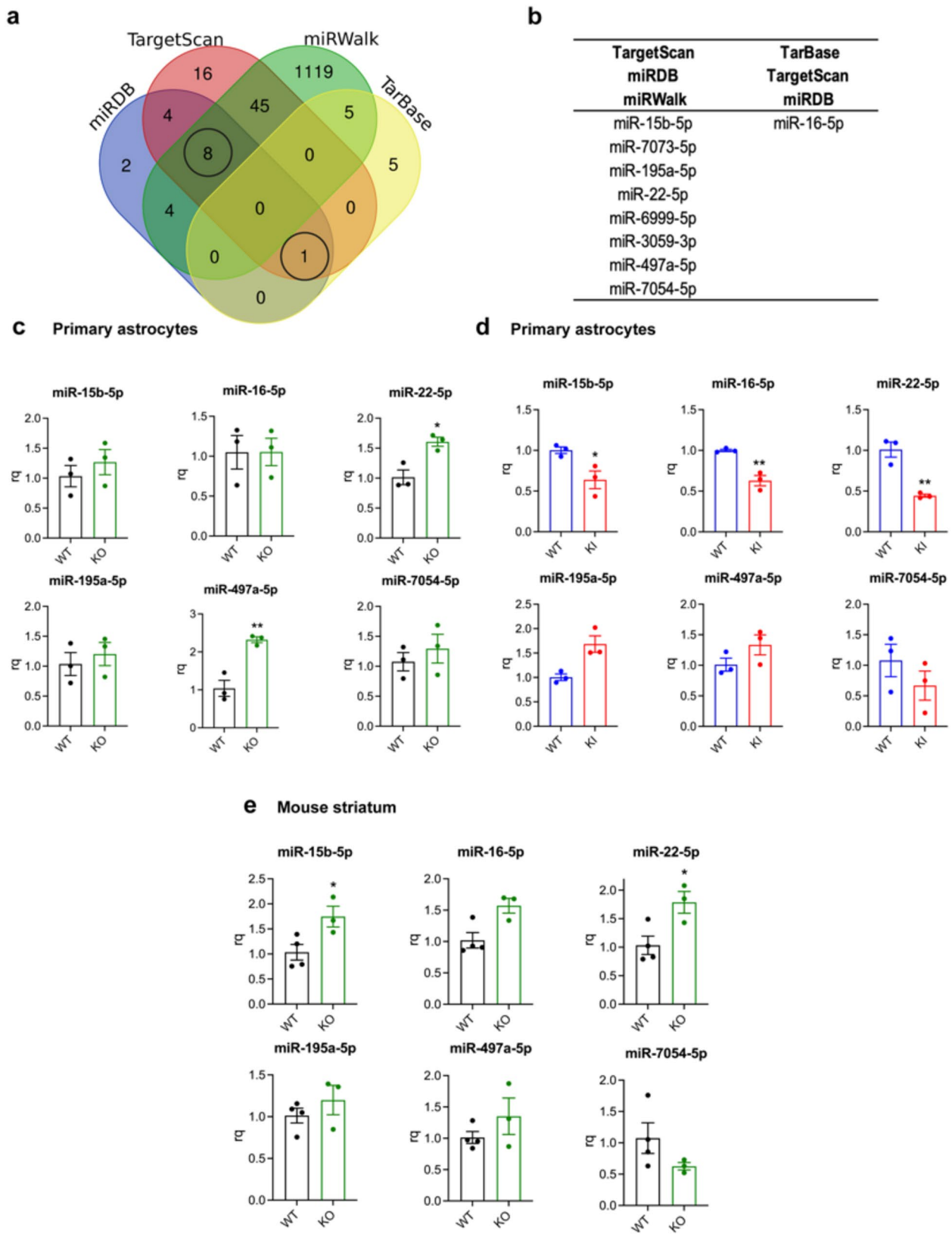


Fig. 6 (See legend on next page.)

(See figure on previous page.)

Fig. 6 Selection and validation of predicted Clu targeting miRNAs. **(a)** Bioinformatics prediction analysis of miRNAs that target Clu mRNA. **(b)** miRNAs identified by at least three databases were selected for further analysis. **(c)** Relative expression of selected miRNAs in LRRK2 KO and WT primary astrocytes normalized on the geometric mean of the reference RNAs and expressed as rq. Data are representative of three independent experiments and are expressed as the mean \pm SEM. Data were analyzed using unpaired t-test, miR-22-5p with $p=0.0145$ and miR-497-5p with $p=0.0047$. **(d)** Relative expression of selected miRNAs in LRRK2 WT and G2019S-KI primary astrocytes normalized on the geometric mean of the reference RNAs and expressed as rq. Data are representative of three independent experiments and are expressed as the mean \pm SEM. Data were analyzed using unpaired t-test, miR-15b-5p with $p=0.0348$, miR-16-5p with $p=0.0045$ and miR-22-5p with $p=0.0039$. While data of miR-195-5p were analyzed using Mann Whitney test. **(e)** Relative expression of selected miRNAs in the striatum of LRRK2 WT and KO mice normalized on the geometric mean of the reference RNAs and expressed as rq. Data are representative of at least 3 animals (LRRK2 WT=4 and KO=3) and are expressed as the mean \pm SEM. Data were analyzed using unpaired t-test, miR-15b-5p with $p=0.0376$ and miR-22-5p with $p=0.0289$. While data of miR-16-5p were analyzed using Mann Whitney test

levels of Clu in astrocytes. Interestingly, by dissecting the molecular mechanism underlying this regulation, we found that LRRK2 G2019S affects preClu expression (and consequently its cleaved forms) at the translational level through the action of miR-22-5p. In addition, we demonstrated that the treatment with miR-22-5p mimic can enhance the ability of LRRK2 G2019S-KI astrocytes to ingest fibrillary α -syn. Overall, our results suggest that LRRK2 G2019S affects α -syn uptake by astrocytes through the Clu-related pathway.

The propagation of α -syn pathological species appears to be one of the main causes of PD pathology [3]. By now, it is well-known that glial cells are able to ingest and clear α -syn aggregates [14]. Recently, astrocytes have attracted particular attention from several points of view since they represent the most abundant glial type in the brain, and their dysfunctions may contribute to the pathogenesis of PD [6]. Multiple studies have shown that astrocytes clear extracellular α -syn [15, 30, 31, 33, 57, 60], thus they can mitigate α -syn spreading and preserve neurons from toxicity [33, 57]. Supporting the crucial role of these cells in the clearance of α -syn, astrocytes have been reported to exhibit α -syn inclusions in the post-mortem brains of PD patients [7, 59]. Despite these interesting results, the intracellular signaling pathway(s) underlying α -syn uptake in astrocytes are still not fully elucidated. Of interest, here we found that PD-linked LRRK2 G2019S enhanced Clu levels in astrocytes, revealing that the inhibition of the LRRK2 G2019S-Clu pathway might improve astrocytic uptake/clearance and potentially limit neuronal α -syn spreading.

We started our study by validating in our mouse strain the impact of the LRRK2 G2019S pathological mutation on α -syn pffs uptake. Specifically, we measured the intracellular amount of pHrodo-labeled α -syn pffs in LRRK2 G2019S-KI primary astrocytes compared to their WT cells. As expected, we found that G2019S-KI astrocytes exhibited a reduced amount of intracellular α -syn. In accordance with our results, primary astrocytes derived from another LRRK2 G2019S-KI mouse strain [23] also displayed attenuated levels of internalized α -syn seeds [54], indicating that the LRRK2 G2019S mutation leads to astrocytes with an impaired ability to ingest aggregated α -syn species. Since we previously demonstrated

that α -syn pffs uptake by astrocytes is hampered by the chaperone Clu [15], here we asked whether LRRK2 G2019S can affect this pathway through Clu. By using *ex vivo* and *in vitro* systems and different approaches, we found that LRRK2 G2019S-KI mouse brains and primary astrocytes exhibited increased Clu levels compared to their respective WT. Accordingly, we observed an opposite effect in brain and primary astrocytes from LRRK2 KO mice compared to their respective WT, confirming that LRRK2 positively controls Clu levels in astrocytes. Trying to understand how LRRK2 G2019S regulates Clu levels, we first analyzed Clu gene expression in LRRK2 G2019S-KI and LRRK2 KO primary astrocytes compared to their control cells, but we did not find any differences, indicating that LRRK2 does not impact Clu gene expression. Then, since LRRK2 has been linked to protein translation process [26, 29, 38, 39], we evaluated whether LRRK2 regulates protein synthesis even in astrocytes. By using the SUnSET assay, we found that LRRK2 positively regulates the global protein translation process also in this cell-type. In this context, multiples studies highlighted that LRRK2 is implicated in the protein synthesis and that dysregulation of translation could be associated to PD pathogenesis [26, 29, 38, 39]. In details, through ribosome profiling studies of global translation, mRNAs with complex 5'UTR structures have been reported to be preferentially translated in the G2019S LRRK2-expressing mouse brains and down-regulated in LRRK2 KO-expressing brains [29]. In another study, Kim and colleagues, specifically showed that in LRRK2 G2019S dopaminergic neurons derived from hiPSC the enhanced translation involved Ca^{2+} homeostasis genes [28], which potentially contribute to the progressive neurotoxicity of dopaminergic neurons in PD. Moreover, LRRK2 has been reported to interact with and phosphorylate ribosomal proteins in *Drosophila* and human neuron PD models [38, 39] and to phosphorylate the translational factor 4E-BP in *Drosophila* [26]. Thus, to gain insight to how LRRK2 G2019S regulates translation in astrocytes, we investigated the 4E-BP pathway; however, we did not find any differences in LRRK2 G2019S-KI astrocytes compared to their WT cells, indicating that LRRK2 does not specifically affect the 4E-BP pathway in astrocytic cells. Taken together, our findings indicate that LRRK2

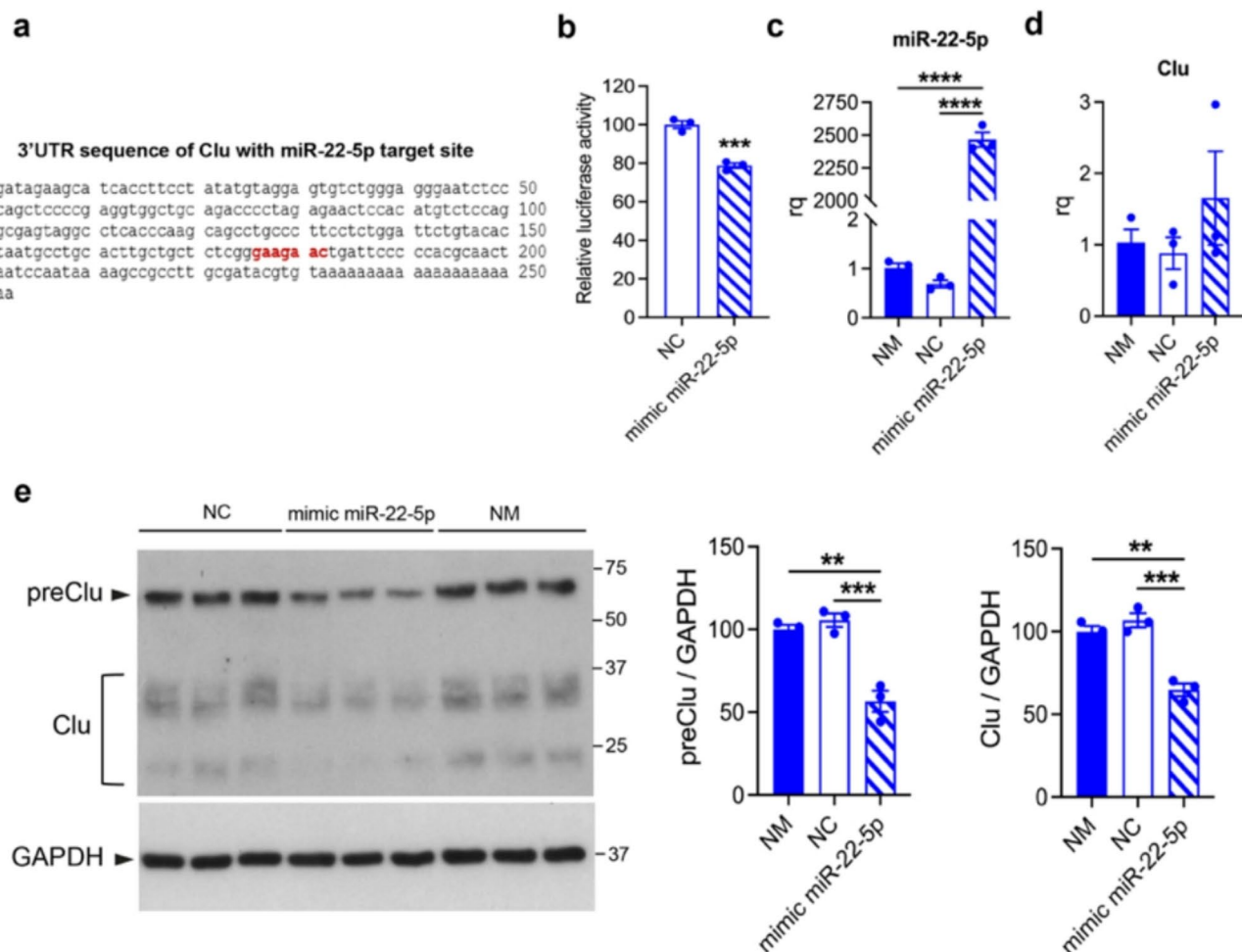


Fig. 7 Clu mRNA is a biological target of miR-22-5p. **(a)** 3'UTR sequence of Clu with indicated miR-22-5p target binding sequence (miRDB database). **(b)** MiR-22-5p-Clu target binding validation assay. Relative luciferase activity was measured in HEK293T cells co-transfected with pmirGLO Dual-Luciferase expression vector containing an approximately 70 bp-long sequence of 3' UTR Clu and with miR-22-5p mimics or NC. Data are representative of three independent experiments and expressed as the mean ± SEM. Data were analyzed using unpaired t-test, $p=0.0008$. **(c)** Quantification of miR-22-5p expression in astrocytes transfected with miR-22-5p mimic or NC. Cells treated with the transfectant agent NM were used as additional control. miR-22-5p expression was normalized on the geometric mean of the reference RNAs and expressed as rq. Data are representative of three independent experiments and expressed as the mean ± SEM. Data were analyzed using one-way ANOVA followed by Tukey's post-hoc test; NC vs. mimic miR-22-5p, $p < 0.0001$; NM vs. mimic miR-22-5p, $p < 0.0001$. **(d)** Quantification of Clu gene expression in astrocytes transfected with miR-22-5p mimic or NC. Cells treated with NM were used as additional control. Clu gene expression was normalized on the geometric mean of the HK genes and expressed as rq. Data are representative of three independent experiments and expressed as the mean ± SEM. Data were analyzed using one-way ANOVA followed by Tukey's post-hoc test. **(e)** Quantification of Clu protein in astrocytes transfected with miR-22-5p mimic or NC. Cells treated with NM were used as additional control. preClu and the cleaved form were normalized on GAPDH. Data are representative of three independent experiments validated on three different primary cultures and expressed as the mean ± SEM. Data were analyzed using one-way ANOVA followed by Tukey's post-hoc test; preClu: NC vs. mimic miR-22-5p, $p=0.0007$; NM vs. mimic miR-22-5p, $p=0.0014$. Clu: NC vs. mimic miR-22-5p, $p=0.0006$; NM vs. mimic miR-22-5p, $p=0.0015$

positively regulates protein translation in astrocytes, and potentially Clu levels, without affecting the translation factor 4E-BP. Overall, the role of LRRK2 in translation remains still unclear, but if LRRK2 G2019S results in a loss of translational control, this might enhance the cell susceptibility to stress that in combination with multiple factors, such as genetics, aging and environment, might lead to disease development.

miRNAs are key regulators of mRNA translation [2] and, of interest, LRRK2 activity has been associated with

this cellular process [18, 19]. Based on these observations, we then explored whether LRRK2 G2019S specifically controls Clu protein levels *via* regulation of microRNAs (miRNAs). Through a bioinformatics prediction analysis, we selected 9 potential miRNAs that target Clu mRNA and, interestingly, some of them (miR-15-b, miR-16b, miRNA 195a and miR-22-5p) have also been correlated with PD pathogenesis [13, 24, 35, 58]. By analysis of the striatum from LRRK2 KO mice and primary astrocytes from LRRK2 KO and G2019S-KI mice, we identified

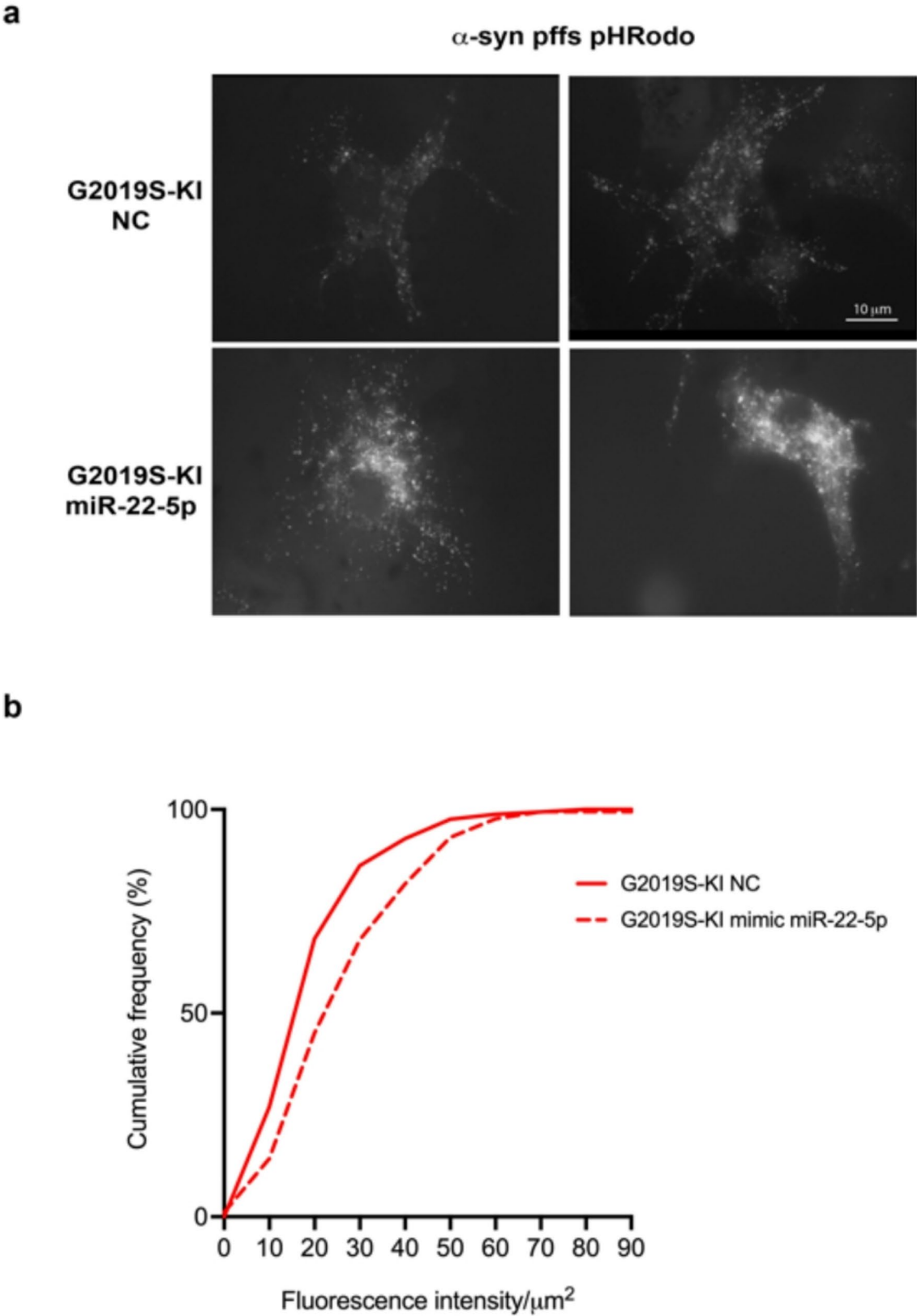


Fig. 8 (See legend on next page.)

(See figure on previous page.)

Fig. 8 Clusterin miR-22-5p increases the ability of LRRK2 G2019S-KI primary astrocytes to take up α -syn pffs. **(a)** Representative fluorescence microscopy images of LRRK2 G2019S-KI astrocytes treated with mouse pHrodo labeled α -syn pffs for 16 h. Scale bar 10 μ m. **(b)** Cumulative frequency distributions of intracellular pHrodo labeled α -syn pffs in LRRK2 G2019S-KI transfected with NC or miR-22-5p mimic (LRRK2 G2019S-KI NC = 167 cells and LRRK2 G2019S-KI miR-22-5p mimic = 175 cells; Kolmogorov-Smirnov test, $p < 0.0001$). Quantification of intracellular α -syn pffs is calculated as fluorescence intensity/ μ m² from three independent experiments (~ 50 cells per experiment)

miR-22-5p as a putative miRNA for Clu regulation. Remarkably, we confirmed that Clu is targeted by miR-22-5p through miRNA target binding validation luciferase reporter assay in HEK293 cells and by overexpressing miR-22-5p mimic in primary astrocytes, where we found a significant reduction of the preClu protein (and consequently its cleaved form). Of relevance, miR-22-5p has been shown to be low expressed in PD blood samples and proposed as potential biomarker for PD [35]. However, a recent study reported increased levels of miR-22-5p in the serum EVs from PD patients [21], thus suggesting that further investigations with high number of samples are required to better understand the link between miR-22-5p and PD pathogenesis. In this study, at the cellular level we demonstrated that the treatment with miR-22-5p mimic enhances the ability of LRRK2 G2019S-KI astrocytes to take up α -syn pffs. Taken together, our results showed that LRRK2-Clu pathway is involved in the ingestion of α -syn fibrils and the impaired ability of LRRK2 G2019S-KI astrocytes to take up α -syn pffs are associated to Clu levels. Interestingly, these observations support the hypothesis that the pharmacological modulation of LRRK2 G2019S-Clu pathway might improve the ability of LRRK2 G2019S astrocytes to take up/clear α -syn aggregates and consequently attenuate the neuron-to-neuron spreading of α -syn pathology in PD. Future in vivo studies performed in LRRK2 G2019S-KI transgenic mice will help to define the implication of the LRRK2-Clu pathway in PD pathogenesis and whether LRRK2 kinase inhibition might attenuate the pathology.

Conclusions

Overall, our study reveals that LRRK2 G2019S augments the levels of Clu protein *via* miRNA-22-5p and that LRRK2 G2019S-Clu pathway impacts the ability of astrocytes to internalize α -syn pffs. Certainly, further investigations are required to shed light on the LRRK2-miR-22-5p-Clu axis and dissect the molecular mechanism underlying LRRK2-mediated Clu regulation.

Abbreviations

PD	Parkinson's Disease
LRRK2	Leucine Rich Repeat Kinase 2
Clu	Clusterin cleaved form
preClu	Clusterin precursor
α -syn	α -synuclein
KO	Knock-out
KI	Knock-in
WT	Wild type
PBS	Phosphate Buffer Saline
DMEM	Dulbecco's Modified Eagle Medium

FBS	Fetal Bovine Serum
DIV	Day in vitro
GFAP	Glial Fibrillar Acidic Protein
RCF	Relative centrifugal force
RT	Room Temperature
Pffs	Pre-formed fibrils
EDTA	EthylenDiaminoTetracetic Acid
SDS	Sodium Dodecyl Sulphate
PVDF	Polyvinylidene difluoride
TBST	Tris Buffered Saline with Tween
GAPDH	Glyceraldehyde-3-phosphate dehydrogenase
HRP	Horseradish Peroxidase
PFA	Paraformaldehyde
DAPI	4',6'-diamidino-2-phenylindole
MMLV-RT	Moloney Murine Leukemia Virus Reverse Transcriptase
dNTPs	Deoxynucleotide Triphosphates
DTT	Dithiothreitol
HKv	Housekeeping
miRNA	microRNA
NM	Neuromag
SUnSET	Surface sensing of translation assay
NC	Negative control
RPKM	Reads per kilobase of transcript per million mapped reads

Supplementary Information

The online version contains supplementary material available at <https://doi.org/10.1186/s40478-025-02015-x>.

Supplementary Material 1

Supplementary Material 2

Acknowledgements

We thank Prof. Luigi Bubacco and Prof. Elisa Greggio, University of Padova, Italy, for kindly providing human α -syn monomeric protein. We are grateful to Dr. Claudia Lodovichi, Neuroscience Institute CNR, Padova, Italy for providing LRRK2 wild-type and LRRK2 knock-out mice to set up the colonies.

Author contributions

AF, GC and IR contributed to the study conception and design. AF and GC performed and analyzed the experiments. AB and MG support the study with resources. AF, GC and IR wrote the manuscript with the inputs from all the authors. All the authors read and approved the final manuscript.

Funding

We are grateful for the financial support of Regional Foundation for Biomedical Research (FRRB, grant ID: 1737591, IR), Cariplo Foundation (grant ID: 2016–0428, IR) and to the Italian Ministry of Health (Ricerca Corrente).

Data availability

The datasets supporting the conclusion of this article are available in the ZENODO repository (<https://doi.org/10.5281/zenodo.12748936>) from the corresponding author upon reasonable request.

Declarations

Competing interests

The authors declare no conflict of interest.

Received: 17 July 2024 / Accepted: 23 April 2025

Published online: 12 May 2025

References

- Albanese F, Mercatelli D, Finetti L et al (2021) Constitutive Silencing of LRRK2 kinase activity leads to early glucocerebrosidase deregulation and late impairment of autophagy in vivo. *Neurobiol Dis* 159. <https://doi.org/10.1016/J.NBD.2021.105487>
- Bartel DP (2004) MicroRNAs: genomics, biogenesis, mechanism, and function. *Cell* 116:281–297. [https://doi.org/10.1016/S0092-8674\(04\)00045-5](https://doi.org/10.1016/S0092-8674(04)00045-5)
- Bieri G, Gitler AD, Brahic M (2018) Internalization, axonal transport and release of fibrillar forms of alpha-synuclein. *Neurobiol Dis* 109:219–225. <https://doi.org/10.1016/j.nbd.2017.03.007>
- Biskup S, West AB (2009) Zeroing in on LRRK2-linked pathogenic mechanisms in Parkinson's disease. *Biochim Biophys Acta - Mol Basis Dis* 1792:625–633
- Bonet-Ponce L, Cookson MR (2021) LRRK2 recruitment, activity, and function in organelles. *FEBS J*. <https://doi.org/10.1111/FEBS.16099>
- Booth HDE, Hirst WD, Wade-Martins R (2017) The role of astrocyte dysfunction in Parkinson's disease pathogenesis. *Trends Neurosci* 40:358–370
- Braak H, Sastre M, Del Tredici K (2007) Development of alpha-synuclein immunoreactive astrocytes in the forebrain parallels stages of intraneuronal pathology in sporadic Parkinson's disease. *Acta Neuropathol* 114:231–241. <https://doi.org/10.1007/s00401-007-0244-3>
- Chen Y, Wang X (2020) MiRDB: an online database for prediction of functional MicroRNA targets. *Nucleic Acids Res* 48:D127–D131. <https://doi.org/10.1093/NAR/GKZ757>
- Choong CJ, Mochizuki H (2022) Neuropathology of alpha-synuclein in Parkinson's disease. *Neuropathology* 42:93–103. <https://doi.org/10.1111/NEUP.12812>
- de Lau LM, Breteler MM (2006) Epidemiology of Parkinson's disease. *Lancet Neurol* 5:525–535. [https://doi.org/10.1016/S1474-4422\(06\)70471-9](https://doi.org/10.1016/S1474-4422(06)70471-9)
- Del Tredici K, Braak H (2016) Review: sporadic Parkinson's disease: development and distribution of alpha-synuclein pathology. *Neuropathol Appl Neurobiol* 42:33–50. <https://doi.org/10.1111/nan.12298>
- di Domenico A, Carola G, Calatayud C et al (2019) Patient-Specific iPSC-Derived astrocytes contribute to Non-Cell-Autonomous neurodegeneration in Parkinson's disease. *Stem Cell Rep* 12:213–229. <https://doi.org/10.1016/J.STEMCELL.2018.12.011>
- Ding H, Huang Z, Chen M et al (2016) Identification of a panel of five serum miRNAs as a biomarker for Parkinson's disease. *Parkinsonism Relat Disord* 22:68–73. <https://doi.org/10.1016/J.PARKRELDIS.2015.11.014>
- Filippini A, Gennarelli M, Russo I (2019) alpha-synuclein and glia in Parkinson's disease: A beneficial or a detrimental duet for the Endo-Lysosomal system?? *Cell Mol Neurobiol* 39:161–168. <https://doi.org/10.1007/S10571-019-00649-9>
- Filippini A, Mutti V, Faustini G et al (2021) Extracellular clusterin limits the uptake of alpha-synuclein fibrils by murine and human astrocytes. *Glia* 69:681–696. <https://doi.org/10.1002/GLIA.23920>
- Filippini A, Gennarelli M, Russo I (2021) Leucine-rich repeat kinase 2-related functions in GLIA: an update of the last years. *Biochem Soc Trans* 49:1375–1384. <https://doi.org/10.1042/BST20201092>
- Foster EM, Dangla-Valls A, Lovestone S et al (2019) Clusterin in Alzheimer's disease: mechanisms, genetics, and lessons from other pathologies. *Front Neurosci* 13:164. <https://doi.org/10.3389/fnins.2019.00164>
- Gehrke S, Imai Y, Sokol N, Lu B (2010) Pathogenic LRRK2 negatively regulates microRNA-mediated translational repression. *Nature* 466:637–641. <https://doi.org/10.1038/NATURE09191>
- Gonzalez-Cano L, Menzl I, Tisserand J et al (2018) Parkinson's Disease-Associated mutant LRRK2-Mediated Inhibition of miRNA activity is antagonized by TRIM32. *Mol Neurobiol* 55:3490–3498. <https://doi.org/10.1007/S12035-017-0570-Y>
- Goodman CA, Hornberger TA (2013) Measuring protein synthesis with sunset: a valid alternative to traditional techniques? *Exerc Sport Sci Rev* 41:107–115. <https://doi.org/10.1097/JES.0B013E3182798A95>
- He S, Huang L, Shao C et al (2021) Several miRNAs derived from serum extracellular vesicles are potential biomarkers for early diagnosis and progression of Parkinson's disease. *Transl Neurodegener* 10. <https://doi.org/10.1186/S40035-021-00249-Y>
- Healy DG, Falchi M, O'Sullivan SS et al (2008) Phenotype, genotype, and worldwide genetic penetrance of LRRK2-associated Parkinson's disease: a case-control study. *Lancet Neurol* 7:583–590. [https://doi.org/10.1016/S1474-4422\(08\)70117-0](https://doi.org/10.1016/S1474-4422(08)70117-0)
- Herzig MC, Kolly C, Persohn E et al (2011) LRRK2 protein levels are determined by kinase function and are crucial for kidney and lung homeostasis in mice. *Hum Mol Genet* 20:4209–4223. <https://doi.org/10.1093/HMG/DDR348>
- Hoss AG, Labadorf A, Beach TG et al (2016) MicroRNA profiles in Parkinson's disease prefrontal cortex. *Front Aging Neurosci* 8. <https://doi.org/10.3389/FNAGI.2016.00036>
- Iannotta L, Bioss A, Kluss JH et al (2020) Divergent effects of G2019S and R1441C LRRK2 mutations on LRRK2 and Rab10 phosphorylations in mouse tissues. *Cells* 9. <https://doi.org/10.3390/cells9112344>
- Imai Y, Gehrke S, Wang HQ et al (2008) Phosphorylation of 4E-BP by LRRK2 affects the maintenance of dopaminergic neurons in *Drosophila*. *EMBO J* 27:2432–2443. <https://doi.org/10.1038/EMBOJ.2008.163>
- Karagkouni D, Paraskevopoulou MD, Chatzopoulos S et al (2018) DIANA-TarBase v8: a decade-long collection of experimentally supported miRNA-gene interactions. *Nucleic Acids Res* 46:D239–D245. <https://doi.org/10.1093/NAR/GKX1141>
- Kim JW, Yin X, Jhaldiyal A et al (2020) Defects in mRNA translation in LRRK2-Mutant hiPSC-Derived dopaminergic neurons lead to dysregulated calcium homeostasis. *Cell Stem Cell* 27:633–645e7. <https://doi.org/10.1016/J.STEM.2020.08.002>
- Kim JW, Yin X, Martin I et al (2021) Dysregulated mRNA translation in the G2019S LRRK2 and LRRK2 Knock-Out mouse brains. <https://doi.org/10.1523/JNEURO.0310-21.2021>. *eNeuro* 8:
- Lee H-J, Suk J-E, Patrick C et al (2010) Direct transfer of alpha-synuclein from neuron to astroglia causes inflammatory responses in synucleinopathies. *J Biol Chem* 285:9262–9272. <https://doi.org/10.1074/jbc.M109.081125>
- Lindström V, Gustafsson G, Sanders LH et al (2017) Extensive uptake of alpha-synuclein oligomers in astrocytes results in sustained intracellular deposits and mitochondrial damage. *Mol Cell Neurosci* 82:143–156. <https://doi.org/10.1016/j.jmcs.2017.04.009>
- Lopes da Fonseca T, Villar-Piqué A, Outeiro T (2015) The interplay between Alpha-Synuclein clearance and spreading. *Biomolecules* 5:435–471. <https://doi.org/10.3390/biom5020435>
- Loria F, Vargas JY, Bousset L et al (2017) alpha-synuclein transfer between neurons and astrocytes indicates that astrocytes play a role in degradation rather than in spreading. *Acta Neuropathol* 134:789–808. <https://doi.org/10.1007/s00401-017-1746-2>
- Maekawa T, Sasaoka T, Azuma S et al (2016) Leucine-rich repeat kinase 2 (LRRK2) regulates alpha-synuclein clearance in microglia. *BMC Neurosci* 17:77. <https://doi.org/10.1186/s12868-016-0315-2>
- Margis R, Margis R, Rieder CRM (2011) Identification of blood MicroRNAs associated to parkinson's disease. *J Biotechnol* 152:96–101. <https://doi.org/10.1016/J.JBIOTECH.2011.01.023>
- Martin I, Dawson VL, Dawson TM (2011) Recent advances in the genetics of Parkinson's disease. *Annu Rev Genomics Hum Genet* 12:301–325. <https://doi.org/10.1146/ANNUREV-GENOM-082410-101440>
- Martin I, Kim JW, Dawson VL, Dawson TM (2014) LRRK2 pathobiology in Parkinson's disease. *J Neurochem* 131:554–565. <https://doi.org/10.1111/JNC.12949>
- Martin I, Kim JW, Lee BD et al (2014) Ribosomal protein s15 phosphorylation mediates LRRK2 neurodegeneration in Parkinson's disease. *Cell* 157:472–485. <https://doi.org/10.1016/J.CELL.2014.01.064>
- Martin I, Abalde-Aristain L, Kim JW et al (2014) Aberrant protein synthesis in G2019S LRRK2 *Drosophila* Parkinson disease-related phenotypes. *Fly (Austin)* 8:165–169. <https://doi.org/10.4161/19336934.2014.983382>
- McGeary SE, Lin KS, Shi CY et al (2019) The biochemical basis of MicroRNA targeting efficacy. *Science* 366. <https://doi.org/10.1126/SCIENCE.AAV1741>
- Miklossy J, Arai T, Guo JP et al (2006) LRRK2 expression in normal and pathologic human brain and in human cell lines. *J Neuropathol Exp Neurol* 65:953–963. <https://doi.org/10.1097/01.jnen.0000235121.98052.54>
- Mingardi J, La Via L, Tornese P et al (2021) miR-9-5p is involved in the rescue of stress-dependent dendritic shortening of hippocampal pyramidal neurons induced by acute antidepressant treatment with ketamine. *Neurobiol Stress* 15. <https://doi.org/10.1016/J.YNSTR.2021.100381>
- Morgan TE, Laping NJ, Rozovsky I et al (1995) Clusterin expression by astrocytes is influenced by transforming growth factor B1 and heterotypic cell interactions. *J Neuroimmunol* 58:101–110. [https://doi.org/10.1016/0165-5728\(94\)00194-5](https://doi.org/10.1016/0165-5728(94)00194-5)
- Paisán-Ruiz C, Lewis PA, Singleton AB (2013) LRRK2: cause, risk, and mechanism. *J Parkinsons Dis* 3:85–103
- Pasinetti GM, Johnson SA, Oda T et al (1994) Clusterin (SGP-2): a multifunctional glycoprotein with regional expression in astrocytes and neurons of the adult rat brain. *J Comp Neurol* 339:387–400. <https://doi.org/10.1002/cne.903390307>

46. Russo I, Berti G, Plotegher N et al (2015) Leucine-rich repeat kinase 2 positively regulates inflammation and down-regulates NF- κ B p50 signaling in cultured microglia cells. *J Neuroinflammation* 12:230. <https://doi.org/10.1186/s12974-015-0449-7>
47. Russo I, Di Benedetto G, Kaganovich A et al (2018) Leucine-rich repeat kinase 2 controls protein kinase A activation state through phosphodiesterase 4. *J Neuroinflammation* 15. <https://doi.org/10.1186/s12974-018-1337-8>
48. Russo I, Kaganovich A, Ding J et al (2019) Transcriptome analysis of LRRK2 knock-out microglia cells reveals alterations of inflammatory- and oxidative stress-related pathways upon treatment with alpha-synuclein fibrils. *Neurobiol Dis* 129:67–78. <https://doi.org/10.1016/j.nbd.2019.05.012>
49. Russo I, Bubacco L, Greggio E (2022) LRRK2 as a target for modulating immune system responses. *Neurobiol Dis* 169:105724. <https://doi.org/10.1016/j.nbd.2022.105724>
50. Satake W, Nakabayashi Y, Mizuta I et al (2009) Genome-wide association study identifies common variants at four loci as genetic risk factors for Parkinson's disease. *Nat Genet* 41:1303–1307. <https://doi.org/10.1038/ng.485>
51. Schmidt EK, Clavarino G, Ceppi M, Pierre P (2009) SUnSET, a nonradioactive method to monitor protein synthesis. *Nat Methods* 6:275–277. <https://doi.org/10.1038/NMETH.1314>
52. Spillantini MG, Schmidt ML, Lee VM et al (1997) Alpha-synuclein in Lewy bodies. *Nature* 388:839–840. <https://doi.org/10.1038/42166>
53. Sticht C, De La Torre C, Parveen A, Gretz N (2018) MiRWalk: an online resource for prediction of MicroRNA binding sites. *PLoS ONE* 13. <https://doi.org/10.1371/JOURNAL.PONE.0206239>
54. Streubel-Gallasch L, Giusti V, Sandre M et al (2021) Parkinson's Disease-Associated LRRK2 interferes with Astrocyte-Mediated Alpha-Synuclein clearance. *Mol Neurobiol* 58:3119–3140. <https://doi.org/10.1007/s12035-021-02327-8>
55. Tong Y, Yamaguchi H, Giaime E et al (2010) Loss of leucine-rich repeat kinase 2 causes impairment of protein degradation pathways, accumulation of alpha-synuclein, and apoptotic cell death in aged mice. *Proc Natl Acad Sci U S A* 107:9879–9884. <https://doi.org/10.1073/PNAS.1004676107>
56. Tremblay ME, Cookson MR, Cuvier L (2019) Glial phagocytic clearance in Parkinson's disease. *Mol Neurodegener* 14
57. Tsunemi T, Ishiguro Y, Yoroioka A et al (2020) Astrocytes protect human dopaminergic neurons from alpha-synuclein accumulation and propagation. *J Neurosci* 40:8618–8628. <https://doi.org/10.1523/JNEUROSCI.0954-20.2020>
58. Uwatoko H, Hama Y, Iwata IT et al (2019) Identification of plasma MicroRNA expression changes in multiple system atrophy and Parkinson's disease. *Mol Brain* 12. <https://doi.org/10.1186/S13041-019-0471-2>
59. Wakabayashi K, Hayashi S, Yoshimoto M et al (2000) NACP/alpha-synuclein-positive filamentous inclusions in astrocytes and oligodendrocytes of Parkinson's disease brains. *Acta Neuropathol* 99:14–20. <https://doi.org/10.1007/PL00007400>
60. Yang Y, Song J-J, Choi YR et al (2022) Therapeutic functions of astrocytes to treat alpha-synuclein pathology in Parkinson's disease. *Proc Natl Acad Sci U S A* 119. <https://doi.org/10.1073/PNAS.2110746119>
61. Yue M, Hinkle KM, Davies P et al (2015) Progressive dopaminergic alterations and mitochondrial abnormalities in LRRK2 G2019S knock-in mice. *Neurobiol Dis* 78:172–195. <https://doi.org/10.1016/j.nbd.2015.02.031>
62. Zimprich A, Biskup S, Leitner P et al (2004) Mutations in LRRK2 cause autosomal-dominant parkinsonism with pleomorphic pathology. *Neuron* 44:601–607. <https://doi.org/10.1016/j.neuron.2004.11.005>

Publisher's note

Springer Nature remains neutral with regard to jurisdictional claims in published maps and institutional affiliations.